Transcritical partially premixed strained flames

L. Pons, N. Darabiha, S. Candel†

Laboratoire EM2C, CNRS and Ecole Centrale Paris,
92295 Châtenay-Malabry, FRANCE
† *also with Institut Universitaire de France*

Abstract

This analysis concerns partially premixed strained flames formed when a rich mixture impinges on an oxidizer stream injected in a transcritical state at a pressure exceeding the critical pressure ($p > p_c$) but at a temperature below the critical value ($T < T_c$). Real gas effects arising under these conditions are represented with a new set of numerical routines (TransChem) covering pressures and temperatures including transcritical states and extending the standard Chemkin package to high pressure and low temperature ranges. Partially premixed oxygen/methane flames fed with transcritical oxygen are investigated in the counterflow configuration. This generic problem is used to unravel a flame structure comprising a gradient layer where transcritical dense oxygen is transformed into supercritical oxygen gas, a non-premixed flame sheet and a premixed flame layer. The high pressure kinetics scheme is first selected by comparing detailed laminar burning velocity calculations with recent measurements of this quantity at elevated pressures. Calculations with two kinetic schemes indicate that the chemical mechanism essentially influences the position of the rich premixed flame but does not change the structure of the diffusion flame and the position of the density gradient layer. When the strain rate ϵ_s is increased the distance of the premixed flame with respect to the stagnation plane diminishes like ϵ_s^{-1}, while the gradient layer distance and diffusion flame thickness change like $\epsilon_s^{-1/2}$. As a consquence the diffusion and premixed flames merge at a high but finite value of ϵ_s. The maximum temperature in the flame is reduced but this effect is relatively small. In the pure oxygen flames considered in this analysis, extinction requires very high strain rates. The proximity of the large density gradient only weakly influences the inner flame structure but chemical conversion only takes place in a region where temperature is high and oxygen is in a supercritical, low density state. A computational case is carried out where the mixture and the oxidizer are injected in a transcritical state. It appears that the flame velocity is strongly affected by the mixture temperature and modifies the stability map of the partially premixed flame. Results obtained in this study can be used to examine more complex flames such as those established in practical coaxial injection geometries used in liquid rocket engines. One may infer that the flame established under such transcritical conditions can sustain the very high velocity gradients existing in the flow and that it can spread in the immediate vicinity of the cold and dense oxygen stream. The gradient layer established in this case acts as a nearly impermeable boundary to the region where chemical conversion takes place.

Keywords: partially premixed flames, transcritical, high pressure, strain rate

Prepared for presentation at EUCASS 2009 as paper EUCASS2009-352

1. Introduction

Many practical combustion systems operate at high pressure. Compression is required to extract work from automotive engines, gas turbines and areo-engines. Momentum is obtained in rocket engines by accelerating high pressure hot gases through a nozzle. The propulsion efficiency generally increases with pressure and the combustor size can be diminished. In liquid rocket engines which

motivate the present analysis, the ambient pressure now typically exceeds 10 MPa reaching values of 40 MPa in high performance devices. In the thrust chamber one of the reactants, usually oxygen, is injected in a transcritical state at a temperature below critical ($T < T_c$) but at a pressure exceeding the critical value ($p > p_c$). In liquid rocket gas generators both reactants are injected in a transcritical state and this might also be the case in future LOx/methane engines. Combustion under such extreme conditions is examined in recent experiments mainly in shear coaxial injector configurations and at pressures of up to 7 MPa exceeding the critical pressure of oxygen. The structure of such flames is now well documented (see [1] and [2] for general reviews of high pressure combustion and [3], [4] for reviews of experimental work on transcritical injection and combustion and related analyses). When the oxygen stream is transcritical while the hydrogen or methane stream is supercritical, experiments [5], [6], [7] indicate that the flame is initially close to the oxygen stream and forms a thin highly wrinkled layer separating fuel and oxidizer. Under these conditions, combustion is essentially of the nonpremixed type and the flame forms a thin sheet separating the reactant streams. Recent experiments on flames established by propellants injected under doubly transcritical conditions [8] indicate that the flame features a peculiar structure with two concentric chemically active layers. This observation is deduced from light emission images which indicate that OH* radiation originates from two distinct conical regions extending from the injector unit. The inner flame sheet situated near the central LOx stream fed by oxygen from the core and methane from the annular stream is similar to flames observed in the case of a single transcritical propellant stream. The outer reactive layer develops near the methane stream boundary and is fed by a rich mixture of methane and oxygen. This structure resembles that of a partially premixed flames (PPF) which comprises a non-premixed flame layer and another reactive front formed by a rich mixture of fuel and oxidizer. This indicates that it would be useful to examine partially premixed flames under transcritical injection conditions. One is naturally led to use strained flames of this type as a model problem. It is also worth recalling, at this point, that strained flames have been extensively employed in turbulent combustion modeling to examine local conditions, determine the structure of flamelets composing the turbulent flame and estimate the reaction rate per unit surface. Such calculations also yield extinction conditions and define the local species distributions. The analysis of strained flames has brought much insight on the turbulent combustion process and is commonly employed to discuss turbulent flame properties. Following the same line of reasoning it is logical to explore the structure of transcritical strained flames. Besides giving information on the turbulent combustion process under transcritical conditions, the analysis of strained flames is also of interest for more fundamental reasons.

Previous studies of PPFs indicate [9] that their structure depends on the fuel type. In hydrocarbon/air flames, fuel is consumed in the rich premixed zone producing intermediates like CO or H_2 which are then consummed in the nonpremixed reaction zone. In hydrogen/air flames, hydrogen is not completely reacted in the rich premixed flame and and a certain amount of this species is converted in the diffusion reaction layer. The PPF response to variations of equivalence ratio and strain rate is well documented [10] [11]. It is known from these studies that changes in equivalence ratio mainly affect the premixed reaction layer which is established at a point where the flow velocity matches the laminar burning velocity. The strain rate, ϵ_s, influences both reaction layers. When ϵ_s is increased the premixed flame moves towards the stagnation plane, the diffusion flame thickness decreases and the maximum temperature reached in this region generally decreases [12]. When the reaction layers are sufficiently close together, they merge into a composite flame. A map [13] plotted as a function of ϕ and ϵ_s identifies domains of existence of multiple reaction layers and merging conditions. Recent studies deal with PPFs at high pressure ($p < 4$ MPa) [10] [14]. Transcritical conditions are however considered in two articles which respectively consider nonpremixed strained flames fed with oxygen/hydrogen or oxygen/methane systems ([15],[16]). It is also worth noting that simulations of turbulent transcritical jets and jet flames have been carried out in the transcritical range [17],[18], [19], but all these studies only consider a single transcritical reactant.

The review of the literature indicates that generic strained flames fed by partially mixed reactants and a transcritical oxidizer stream have not been investigated previously. The aim of the present analysis is to analyze this case by developing simulations for the methane/oxygen reactant mixture when the ambient pressure is high and for an oxygen stream injected at a temperature lower than its critical value ($T_{O2} < T_c$). Under these conditions the density of oxygen is high and of the same order of magnitude as that of a liquid. One expects to find a region of rapid density change, a feature which is already present in previous calculations of strained nonpremixed transcritical flames. The constant strain rate is specifically considered because it is a generic problem allowing detailed calculations in a one dimensional framework. This characteristic of strained flows has been extensively exploited in the past mainly to deal with flames formed by perfect gases. This property is is exploited in the present article to examine transcritical features. The modeling of the flow (section 2) relies on a unified treatment of the real gas behaviour of high pressure fluids from transcritical

to supercritical state. This is achieved by making use of numerical routines gathered in a library designated as TransChem which extends the Chemkin package to deal with high pressure low temperature conditions. This is only briefly summarized because the basic elements are already covered in previous articles and the TransChem package is described in [16]. One important aspect when dealing with partially premixed flames is the selection of the kinetic scheme. It is known (for example [20]) that this scheme notably influences the calculated PPF structures. This point is examined in section 3 with simulations based on two schemes. The structure and response of transcritical PPFs to premixedness and strain rate are analyzed in section 4.

2. Flow modeling under transcritical conditions

Calculations of transcritical flames requires a suitable description of thermodynamics functions and transport properties for high pressure fluids which should cover a wide range of temperatures extending from below the critical value to well above that value. There are many aspects which need to be considered to deal with high pressure effects on single and multi-species fluids. These aspects are only synthesized in what follows. In practice, it is convenient to modify a standard library of numerical routines developed for perfect gases like Chemkin to take into account real gas effects on thermodynamics and transport. This is achieved by a library designated as TransChem which uses Chemkin as a subset and extends it to cover broader ranges of pressure and temperature where real gas effects and transport anomalies are important. This development is described in further detail in Ref. [16] and will not be repeated here. We only briefly outline some of the models. One central issue is the choice of a state equation. It is now well established that the state of transcritical fluids can be suitably described by the modified Peng-Robinson equation [21] :

$$p = \frac{RT}{V-b} - \frac{a(T)}{V(V+b)+b(V-b)} \tag{1}$$

where R is the perfect gas constant, T is the temperature, V is the molar volume and where $a(T)$ depends on temperature, critical pressure and temperature p_c and T_c and b depends on p_c and T_c as well :

$$a(T) = 0.45724\frac{R^2T_c^2}{p_c}\alpha(T), \quad b = 0.0778\frac{RT_c}{p_c} \tag{2}$$

where T_c and p_c are respectively the critical temperature and pressure of the considered species and $\alpha(T)$ is defined by :

$$\alpha(T) = 1 + m\left[1 - (T/T_c)^{1/2}\right] \tag{3}$$

where m is given in terms of the acentric factor ω accounting for the polarity of the species : $m = 0.37464 + 1.54226\omega - 0.26992\omega^2$. Mixtures of real gases are conveniently represented by mixing rules. Thermodynamic functions are determined with the departure function method [21]. A typical variable F is obtained by correcting the standard state to account for real gas effects represented by the Peng-Robinson equation. The departure function F_{PR} corresponds to the deviation of the real gas with respect to the reference perfect gas superscripted 0 : $F = F_{PR} + F^0$. Typical results (Fig. 1) show the density of oxygen and methane over a wide range of temperatures at a pressure of 10 MPa. Calculations are close to NIST data [22] over the useful range of temperatures. The modified Peng-Ronbinson equation accurately represents oxygen, methane and other species. Since many of the minor species involved in the combustion process only appear in the high temperature low-density region where the flame is established [16] they behave like perfect gases and it is not necessary to represent their real gas properties.

Transport anomalies related to real gas behavior are reviewed in [23]. Viscosity of transcritical fluids is well represented by a model derived from [24]. This relies on the Chapman-Enskog theory for dilute gases with an added correction taking into account high pressure effects. Viscosity is given by $\mu = \mu^0\mu^*$, where μ^0 is the low pressure viscosity and μ^* is the high pressure correction term. Calculated viscosities are in excellent agreement with NIST data for the range of pressures of interest. According to [23] the thermal conductivity at high pressure is best predicted by an extension of the corresponding states theory (CST) [25] [26]. Thermal conductivity is obtained from $\lambda = \lambda' + \lambda''$ where λ', describes transfer of energy by collisional or translational effects and λ'' pertains to internal degrees of freedom transfer of energy. Calculated thermal conductivities at pressures above critical closely follow NIST data. The modeling of binary diffusion coefficients is more challenging because experimental data is scarce. Coefficients D_{ij}^0 are first estimated at low pressure with the standard transport library [27] and high pressure effects are included by applying corrections

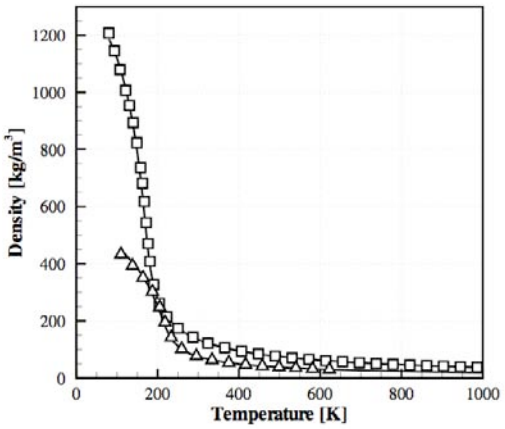

Fig. 1: **Evolution of the density of methane and oxgen for a pressure of 10 MPa over a range of temperatures including transcritical and supercritical states – solid : modified Peng-Robinson equation of state, □ : NIST data for oxygen, △ : NIST data for methane.**

devised by the Takahashi [28] $D_{ij} = D^0_{ij} f(\theta_R, \pi_R)$ where θ_R and π_R respectively designate temperature and pressure normalized by the critical values. The previous treatment was implemented as a set of routines in TransChem [16] describing real fluid behavior for pure species or mixtures over wide ranges of pressures and temperatures. Chemkin is used as a kernel [27] [29] to estimate properties in the standard state where the fluid behaves like a perfect gas.

The balance equations applicable to the reactive flow need to be modified to take into account real gas effects. This problem is tackled in [30] with a general treatment of real fluids in combination with preconditionning schemes. The energy balance in [30], formulated in terms of temperature features many additional terms. In the present treatment, the complexities of the temperature equation are avoided by making use of the enthalpy formulation of the energy balance. Real fluid thermodynamics only appear in the determination of the mixture and species enthalpies h and h_k $(k = 1, N)$. This alternative formulation has been validated by checking that it provides results which are identical to those determined with the standard set of expressions for counterflow flames of perfect gases. The system of equations which is solved takes the form given in equations 4 to 7 (see for example [12]). As indicated the energy equation is written in enthalpy form (eq. 7).

$$\rho\epsilon_s\widehat{U} + \frac{\partial(\rho v)}{\partial z} = 0 \tag{4}$$

$$\epsilon_s(\rho\widehat{U}^2 - \rho_{+\infty}) + \rho v\frac{\partial\widehat{U}}{\partial z} - \frac{\partial}{\partial z}\left(\mu\frac{\partial\widehat{U}}{\partial z}\right) = 0 \tag{5}$$

$$\rho v\frac{\partial Y_k}{\partial z} + \frac{\partial}{\partial z}\left(\rho Y_k V_k\right) - \omega_k W_k = 0\,, \qquad (k = 1, ..., N) \tag{6}$$

$$\rho v\frac{\partial h}{\partial z} - \frac{\partial}{\partial z}\left(\lambda\frac{\partial T}{\partial z}\right) + \frac{\partial}{\partial z}\left(\sum_{k=1}^{N}\rho Y_k h_k V_k\right) = 0 \tag{7}$$

The temperature and composition is specified at the boundaries of the domain and the calculation is carried out for an imposed value of the strain rate (ϵ_s) which is used to specify conditions on the flow velocity. At the $z = -\infty$ boundary, species are given by $Y_k = Y_{k,-\infty}$, temperature by $T = T_{-\infty}$, and the reduced velocity $\widehat{U}$ by $\widehat{U} = \left(\frac{\rho_{+\infty}}{\rho_{-\infty}}\right)^{1/2}$. On the other side, at $z = +\infty$, species are given by $Y_k = Y_{k,+\infty}$, temperature by $T = T_{+\infty}$, and the reduced velocity by $\widehat{U} = 1$. The last boundary condition concerns the stagnation plane ($z = 0$) where the velocity equals zero.

3. Numerical details and influence of kinetics

Calculations carried out in this study correspond to partially premixed strained laminar flames formed by low temperature oxygen impinging on a methane/oxygen mixture in a 7 MPa environment (Fig. 2). This pressure is used because it is approximately equal to

that prevailing in the model scale experiments carried out with transcritical oxygen and gaseous hydrogen and gaseous or transcritical methane. On the oxidizer side, at $z = -\infty$, $T = 80$ K, $Y_{O2} = 1$. At $z = +\infty$, $T = 300$ K, the methane/oxygen mixture has an equivalence ratio ϕ. The flow features a diffusion flame (DF), a rich premixed flame (PF) on the methane/oxygen side and a gradient layer where the dense transcritical oxygen is transferred into a light supercritical form of this substance. The set of equations corre-

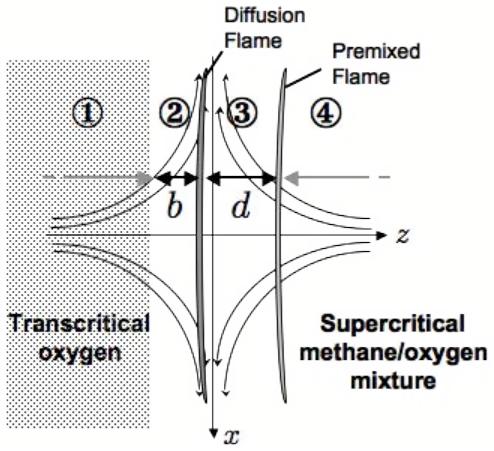

Fig. 2: **Partially premixed strained flame formed by transcritical oxygen and supercritical rich methane / oxygen mixture.**

sponding to an imposed strain rate formulation is standard, except for the treatment of the energy equation, and is given in equations 4 to 7. The computational domain is dynamically rescaled and a new mesh is generated to accomodate gradients and rapid changes in these gradients. Real gas thermodynamics and transport properties are obtained from the TransChem library discussed previously while complex chemistry is handled with the Chemkin package [29].

One difficulty in PPF modeling is to accurately reproduce the structures of both non-premixed and rich premixed flames. The kinetic scheme influence on the structure of this type of flames is first examined by considering PPFs where both reactants are injected above their critical temperature ($T_{O2} = 300$ K) and comparing the GRI-Mech 3.0 [31] and Lindstedt mechanisms [32] [33]. It is known [34] that these two mechanisms give similar results for high pressure nonpremixed flames formed by pure methane and pure oxygen.

Partially premixed flames structures calculated with the two mechanisms are compared in Fig. 3 in the case of supercritical injection of oxygen and a methane/oxygen mixture featuring two equivalence ratios and a strain rate of 10^3 s^{-1}. The diffusion flame is located close to the stagnation plane, $z = 0$ with a peak temperature situated on the oxygen side. The premixed front is established on the right of the stagnation plane, at $z = 6$ mm for $\phi = 1.7$ and around $z = 0.8$ mm for $\phi = 3$. As expected, the kinetic schemes provide similar profiles for the diffusion flame, but the premixed flame location changes with the mechanism when $\phi = 3$. One finds that the flame structure, in terms of species and temperature, does not change.

In the present context, it is important to examine rich premixed methane/oxygen flames and compare the two schemes by calculating laminar burning velocities at high pressure. This is achieved by the use of the PREMIX code [35] comparing GRI-Mech 3.0 and Lindstedt, called L-98 for the rest of the paper, mechanisms with experimental data. First, the performances of the two schemes are tested on high pressure helium-diluted methane/oxygen flames. Rozenchan et al. [36] report results of experiments on methane/oxygen/helium (15% O_2) premixed flames at 60 atm and provide laminar burning velocity measurements as a function of the equivalence ratio. Figure 4 displays the laminar burning velocity of premixed flames, under conditions given previously, for equivalence ratios from 0.8 to 1.4. The GRI-Mech scheme gives good results for equivalence ratios up to 1.2 but beyond this value, the L-98 mechanism is more effective. In the case of partially premixed flames, the premixed flame is very rich, so that the equivalence ratio reaches values as high as 3. From the results given in Fig. 4, one can expect that the L-98 scheme would be the more accurate to simulate high pressure, rich premixed diluted oxygen/methane flames.

In the applications considered in this paper, flames are fed by pure oxygen and pure methane. One has therefore to consider the kinetic schemes response for the determination of laminar burning velocity of pure oxygen / pure methane premixed flames. This is

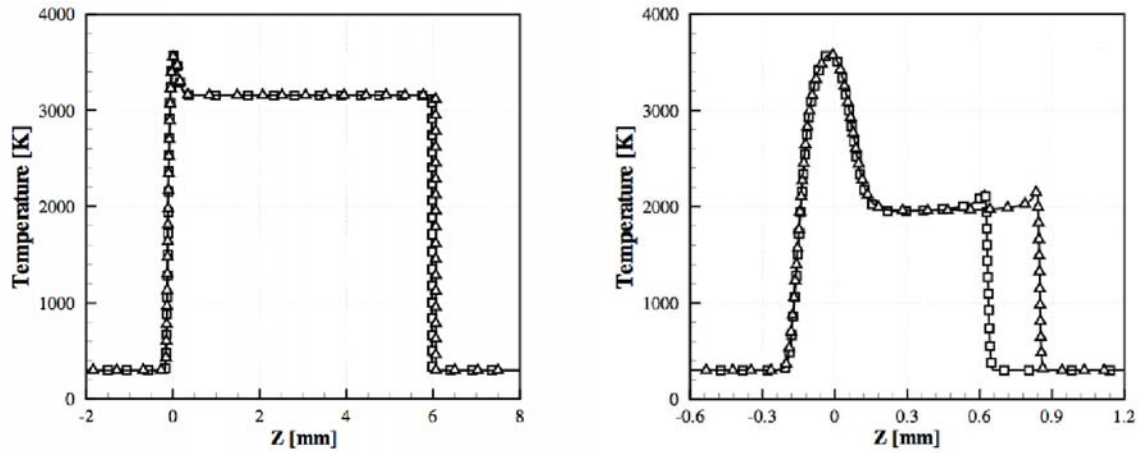

(a) $\phi = 1.7$ (b) $\phi = 3$

Fig. 3: **Comparison of the structure of partially premixed strained flames.** p **=7 MPa. Oxygen (left) and methane/oxygen mixture (right) are injected at 300 K.** $\epsilon_s = 1000\ \mathbf{s}^{-1}$**. (a)** $\phi = 1.7$**, (b)** $\phi = 3$**.** $\square$**: Lindstedt,** $\triangle$**: GRI-mech 3.0.**

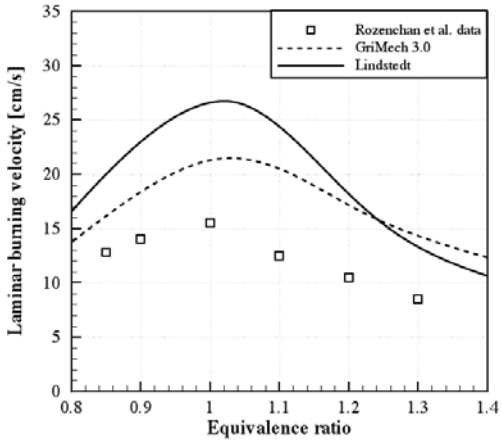

Fig. 4: **Laminar burning velocity of freely-propagating methane/oyxgen/helim (15% O_2) premixed flames at 60 atm and where reactants are injected at 300 K with** ϕ **varying from 0.8 to 1.4. solid : Lindstedt mechanism, – – : GRI-mech 3.0,** $\square$**: experimental data from [112]**

what is done in the results displayed in Fig. 5. GRI-Mech 3.0 and L-98 mechanisms are compared in the calculation of the laminar burning velocity of a methane/oxygen/nitrogen (98.5% O_2) flame in a 1 atm environment with the experimental data from [37] [38]. The GRI-Mech scheme underestimates the laminar flame speed over the whole range of methane percentage considered. On the other hand, the L-98 scheme narrowly follows the experimental data over the whole operating range.

The Lindstedt L-98 mechanism is shown to provide a good representation of non-premixed methane/oxygen flames at high pressure [34]. Calculations, carried out for high-pressure diluted methane/oxygen premixed flames and of a pure methane/pure oxygen atmospheric premixed flames, demonstrate that the L-98 scheme gives the most accurate estimation of the laminar burning velocity. In partially premixed strained flames, this quantity governs the location of the premixed sheet stabilization. The Lindstedt scheme, also being more computationally efficient, it is chosen in what follows to calculate transcritical PPFs.

4. Results and discussion

The counterflow is formed by a stream of pure oxygen injected at $T_{-\infty}$ =80 K impinging on a rich methane/oxygen mixture injected

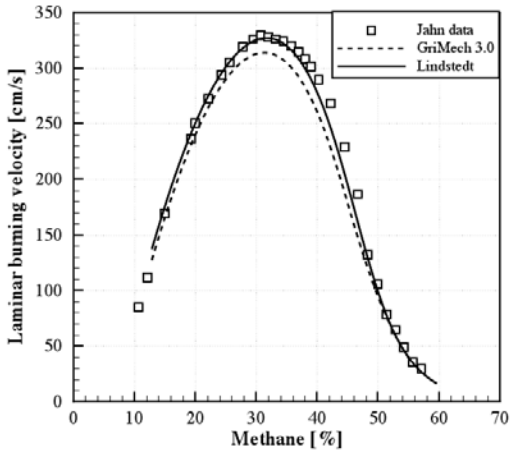

Fig. 5: **Laminar burning velocity of freely-propagating methane/oyxgen/nitrogen (98.5% O_2) premixed flames at 1 atm and where reactants are injected at 300 K with the methane percentage warying from 5 to 55%. solid : Lindstedt mechanism, – – : GRI-mech 3.0, □ : experimental data from Jahn [54] [68]**

at T_∞ =300 K in a 7 MPa environment (Figure 6). This configuration is used to examine the flame structure and response to changes in equivalence ratio and strain rate. The PPF corresponding to an oxygen temperature $T_{-\infty}$ =300 K is also plotted to allow direct comparison. Figure 6 shows the temperature, axial velocity and density profiles in a PPF submitted to a strain rate of $\epsilon_s = 10^4$ s^{-1}. In

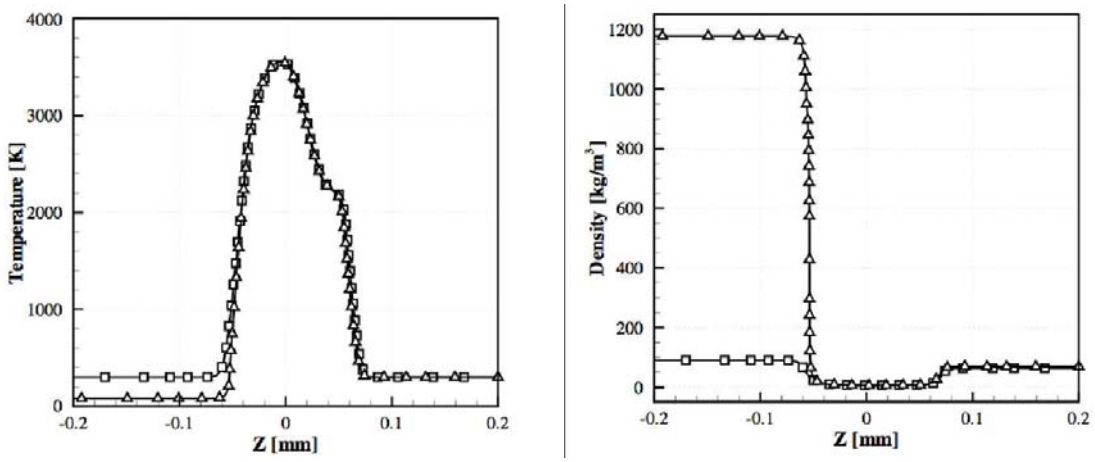

(a) Temperature (b) Density

Fig. 6: **Temperature (a) and density (c) in a PPF formed by a methane / oxygen mixture at 300 K (right) impinging on a transcritical or supercritical oxygen stream (left).** p **=7 MPa.** $\phi = 3$**,** $\epsilon_s = 10^4$ **s**$^{-1}$**.** □ **:** $T_{O_2} = 300$ **K,** △ **:** $T_{O_2} = 80$ **K.**

this case ϕ equals 3 which corresponds to a methane mass fraction $(Y_{CH4})_\infty$=0.428. The oxygen content at ∞ is in this case $(Y_{O2})_\infty$= 0.572. This PPF features standard reaction layers including a rich premixed flame and a non-premixed sheet. Transcritical injection of oxygen is visible in Fig. 6c through a steep density gradient on the oxidizer side of the diffusion flame. The oxygen density at injection reaches a high value of 1176 kg m^{-3} in the initial stream. The density drops sharply at a point where the temperature begins to rise. As for transcritical non-premixed flames [16], the reaction layers are located in the low-density region. The axial velocity profile, displayed in Fig. 6b, indicates that under transcritical injection of oxygen, the reaction layers are shifted towards the stagnation plane. The oxygen jet remains intact deeper in the domain of calculation, because it is in a transcritical state and its transport properties

are notably modified compared to those prevailing in the gaseous case. As in other recent studies it is found that under transcritical injection [16] [19] the density gradient constrains the flame. In the case shown in Fig. 6, the position of the density gradient defines the mass transfer rate from the dense oxygen stream to the light oxygen region feeding the flame. Mass transferred through the density gradient layer must be equal to the consumption rate of oxygen at the flame. The premixed flame is only slightly affected by changes in the oxygen injection temperature because the burning velocity mainly depends on conditions prevailing in the gaseous stream.

Figure 7 displays profiles of temperature, reduced heat release rate distribution $\tilde{Q}(z)$ and density at a strain rate $\epsilon_s = 10^3$ s^{-1} for

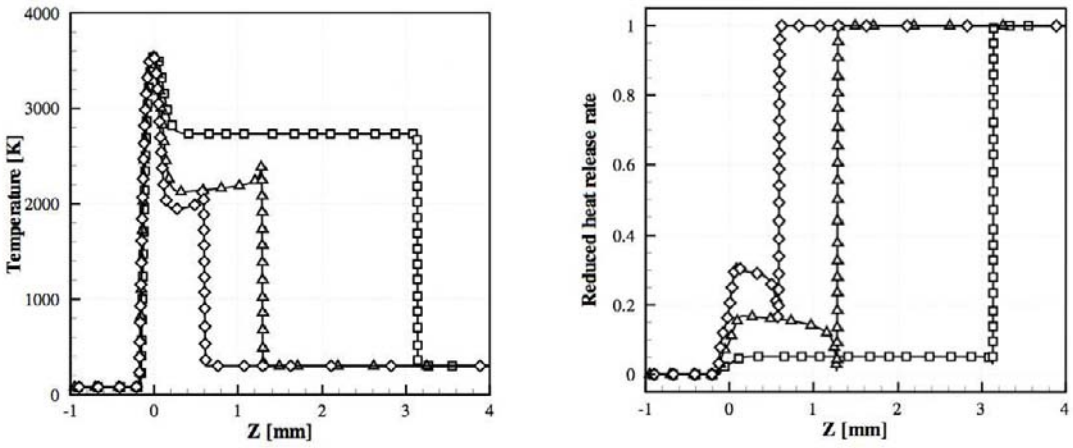

(a) Temperature (b) Reduced heat release rate

Fig. 7: **Temperature (a) and reduced heat release rate distribution (b) in a PPF formed by a methane / oxygen mixture at 300 K impinging on a transcritical oxygen jet at 80 K.** p **=7 MPa.** $\epsilon_s = 1000$ **s**$^{-1}$**.** $\square$ **:** $\phi = 2$**,** $\triangle$ **:** $\phi = 2.5$**,** $\diamond$ **:** $\phi = 3$**.**

three equivalence ratios. The distribution $\tilde{Q}(z)$ is obtained by summing the rates of volumetric heat release from $-\infty$ to the local coordinate z :

$$Q(z) = -\int_{-\infty}^{z} h_k W_k \omega_k dz \tag{8}$$

and dividing by the sum taken over the whole field: $\tilde{Q}(z) = Q(z)/Q(+\infty)$. This variable directly yields an estimate of the amount of heat released per unit surface in the different reactive layers in the flame and can be used to measure the respective contributions of the premixed and non-premixed flames to heat release. Changes in equivalence ratio ϕ of the methane/oxygen mixture, essentially affect the premixed reaction zone. The corresponding reaction front is established at the location where the local velocity equals the laminar burning velocity. An increase in equivalence ratio from 1.7 to 3 reduces the laminar burning velocity shifting the premixed flame towards the stagnation plane where the local flow velocity is lower. The diffusion flame is established at a point where the fluxes of oxidizer and fuel are in stoichiometric proportions which in this case is close to the stagnation plane. This is only slightly affected by changes in equivalence ratio : when varying ϕ from 1.7 to 3, the diffusion flame remains near the same location.

The response to changes in strain rate ϵ_s is examined at an equivalence ratio $\phi = 3$. Figure 8 displays profiles of density, temperature, and reduced heat release rate distribution for flames submitted to moderate to high values of ϵ_s. Figure 8c indicates that, on the oxygen side, the strong density gradient which constrains the flame approaches the stagnation plane. The strain rate is found to affect both reaction layers. A change in ϵ_s implies a modification of the flow velocity field, and the premixed flame stabilizes at a place where the new velocity distribution matches the laminar burning velocity. As the strain rate is increased, the premixed flame moves towards the stagnation plane while the maximum flame temperature in the diffusion flame diminishes, due to the decrease of the residence time in the flame [10] [12]. The thickness also decreases as ϵ_s increases [34].

When the strain rate is high enough, DF and PF layers merge and the PPF resembles a diffusion flame. The temperature profile, in Fig. 8a, displays two distinct reaction layers for $\epsilon_s = 10^3$ s^{-1}, and as the strain rate increases, the premixed and diffusion flames interact and eventually combine. However, two sources of heat release are present, a sharp peak corresponding to the premixed flame, a broader region defining the diffusion flame. This is clearly apparent in the reduced distributions of heat release rate per unit

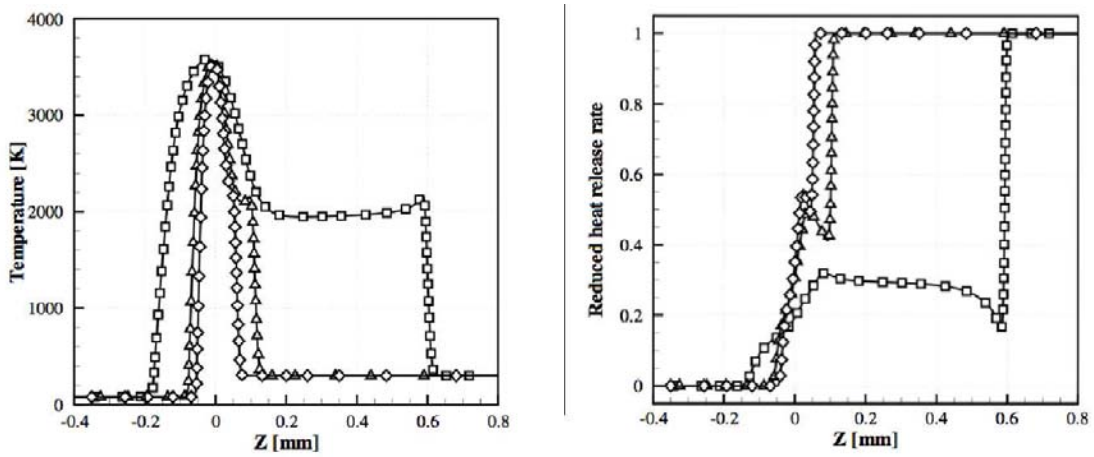

(a) Temperature (b) Reduced heat release rate

Fig. 8: **Temperature (a) and reduced heat release rate distribution (b) in a partially premixed strained flame formed by a methane / oxygen mixture jet at 300 K impinging on a transcritical oxygen jet at 80 K at 7 MPa.** $\phi = 3$**.** $\square$**:** $\epsilon_s = 1000\ \mathbf{s}^{-1}$**,** $\triangle$**:** $\epsilon_s = 5000\ \mathbf{s}^{-1}$**,** $\diamond$**:** $\epsilon_s = 10^4\ \mathbf{s}^{-1}$**.**

surface plotted in Fig. 8b. As ϵ_s increases, the heat released in the diffusion flame is augmented while that of the premixed flame remains constant. The rate of conversion in the premixed flame is essentially determined by the laminar burning velocity $Q_{PF} = \rho_\infty Y_{O\infty} S_L \Delta h$ where Δh is the heat released per unit mass of oxygen ($\Delta h = 12.5$ MJ kg^{-1}). Q_{PF} does not change significantly with the strain rate. Far from extinction the rate of heat release in the diffusion flame scales like $\epsilon_s^{1/2}$ a well known result which can be proved by making use of the fast chemistry limit but which is also obtained for finite chemistry flames when the operating point is far from extinction [34] : $Q_{DF} = \rho Y_{O2-\infty}(1+\Phi)(D\epsilon_s/2\pi)^{1/2}\exp(-\eta_f^2)\Delta h$ where Φ is the global mixture ratio which compares the fuel/oxidizer ratio to the mass stoichiometric coefficient s of the methane/oxygen reaction and $\mathrm{erf}(\eta_f) = (1-\Phi)/(1+\Phi)$. Here $Y_{O2-\infty} = 1$ and it is possible to approximate Φ by $\Phi = s(\phi-1)/(s+\phi)$. The previous expressions indicate that the premixed and non-premixed flames produce the same amount of heat per unit surface for $\epsilon_s \simeq 10^4$ s^{-1} and numerical calculations confirm this estimate as can be seen in Fig. 8b.

The structure of partially premixed flames is naturally characterized by the distance b separating the two reaction layers (Fig. 2). This scale can be used to determine the merging limit and establish a map of possible regimes. In the case of transcritical injection of one of the reactants, it is also interesting to determine the distance d separating the density gradient and the diffusion flame (Fig. 2). When this scale vanishes the gradient layer merges with the diffusion flame and the internal flame structure is modified. If this distance remains finite, the diffusion flame is weakly influenced by the presence of the dense oxygen stream but the flame is constrained to lie on the low density side of the gradient layer. The distances d and b can be deduced from Fig. 9 which shows positions of the density gradient layer, non-premixed and premixed reaction layers for an equivalence ratio $\phi = 3$ plotted as a function of the strain rate ϵ_s between 10^3 s^{-1} and 4 10^4 s^{-1}. The peaks in HO_2 profile serve as indicators of reactive layers and define their positions with respect to the stagnation plane. In the range of strain rates considered in Fig. 9 there are two peaks indicating the presence of two reaction layers. The density gradient location is defined by the z-coordinate where the temperature equals the critical value $T = T_{cO2}$. As the strain rate increases, the premixed reaction layer moves towards the stagnation plane and its location evolves like $1/\epsilon_s$. The non-premixed reaction layer and the density gradient layer also move towards the stagnation plane and their positions changes like $\epsilon^{-1/2}$. The two reaction layers merge when the strain rate reaches 4 10^4 s^{-1}. The HO_2 profile still features two peaks but the temperature distribution is closer to that of a non-premixed flame. When the strain rate is augmented still further above the merging value the flame response is dominated by the diffusion flame. In that case the heat release per unit surface area increases like $\epsilon_s^{1/2}$ while the maximum temperature diminishes, eventually leading to flame extinction where these two quantities drop sharply. In the case of a flame fed by a transcritical reactant, one may wonder whether the proximity of the low temperature stream modifies the flame response to strain

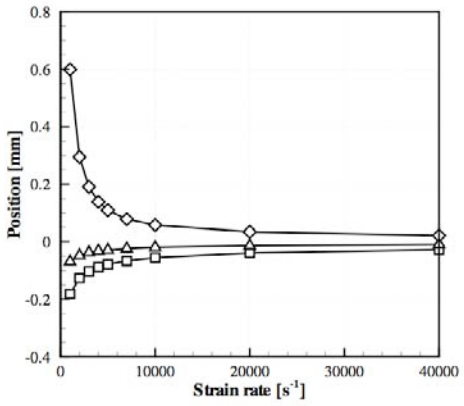

Fig. 9: **Positions of the premixed flame (◇), non-premixed flame (△) and density gradient (□) as a function of the strain rate. The PPF is formed by a methane / oxygen mixture injected at 300 K impinging on a transcritical oxygen stream at 80 K.** p **=7 MPa.** $\phi = 3$**.**

rate. The maximum temperature is calculated as a function of the strain rate for a gaseous and a transcritical PPF at 7MPa and $\phi = 3$. The flame temperature is lowered by transcritical injection. As strain rate increases, the maximum temperature of the transcritical PPF is always lower than that of the gaseous flame and the difference increases as the gradient layer approaches the diffusion flame. One can expect that the transcritical flame will be extinguished at a lower strain rate than that characterizing a gaseous flame. However, pure oxygen flames are quite robust and their extinction takes place at very high strain rate values. This indicates that in the coaxial injection configuration used in rocket engines the flame can sustain the large strain rates existing in the flow and that the reactive layer can develop in the near vicinity of the dense transcritical reactant with an internal structure quite similar to that of a gaseous flame.

It is now interesting to consider a partially premixed strained flame where both the oxygen and the oxygen / methane mixture are injected at a temperature below critical. This case can be used to approach conditions prevailing when a flame is formed by coaxial injection of two transcritical reactants. This case is documented in some recent experiments of Singla et al. [8]. In the flame formed between transcritical oxygen and transcritical methane one finds two concentric chemically active layers. The first is established in the near vicinity of the oxygen jet and corresponds to a diffusion flame layer, the second is observed near the outer boundary of the methane jet and indicates that some mixing has taken place between the transcritical streams of methane and oxygen and that this yields a rich premixed flame. It is then logical to consider a strained flame formed between a transcritical stream of pure oxygen and a rich transcritical mixture of methane and oxygen. For this calculation, the pressure is kept constant at 7 MPa, pure oxygen is injected at $z = -\infty$ at 80 K and the oxygen / methane mixture is injected at $z = +\infty$ at 110 K. This value is well below the critical temperatures of both species forming the mixture and is also below the critical temperature of the mixture. The strain rate is low and fixed at a value of 50 s^{-1}.

The flame structure obtained under these extreme injection conditions is displayed in Fig. 10 and is compared with a supercritical partially premixed flame (injection temperatures : 300 K) at the same strain rate. On the oxygen side, the flame is slightly shifted towards the stagnation plane. This is due to transcritical injection of the reactant wich reduces mass diffusion. The maximum flame temperature (Fig. 10(a)) is also slightly diminished because the reactants are injected at a lower temperature. A noticeable phenomenon is the shift of the premixed flame towards the stagnation plane when the injection temperature of the mixture decreases. This has been observed previously in the experiments of Zitoun and Deshaies [39] who considered rich mixture of H_2 / O_2 at cryogenic temperature and investigated the influence of the fresh mixture temperature on the burning velocity. It was found that, to a first approximation, the laminar burning velocity decreases in a linear way with the fresh mixture temperature. One finds in Fig. 10 that the premixed flame is stabilized closer to the stagnation plane when the injection temperature diminishes which confirms that the burning velocity decreases with the temperature. During the transition from the super- to transcritical state, the evolution of the burning velocity is not linear, a small variation in temperature induces a large burning velocity change. The strain rate considered in this calculation is quite low so

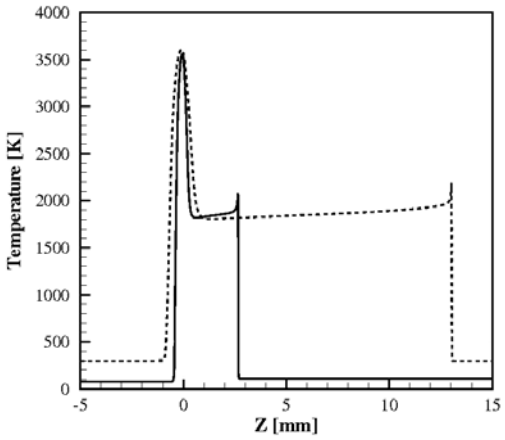

(a) Temperature

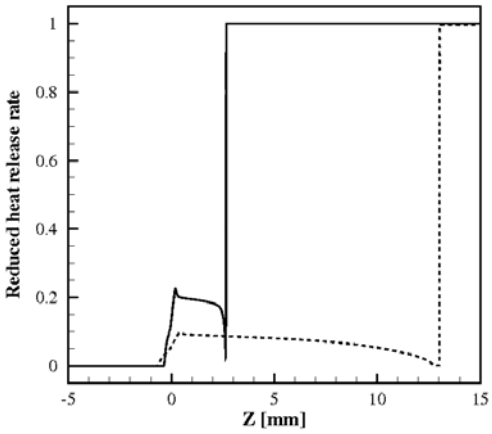

(b) Reduced heat release rate

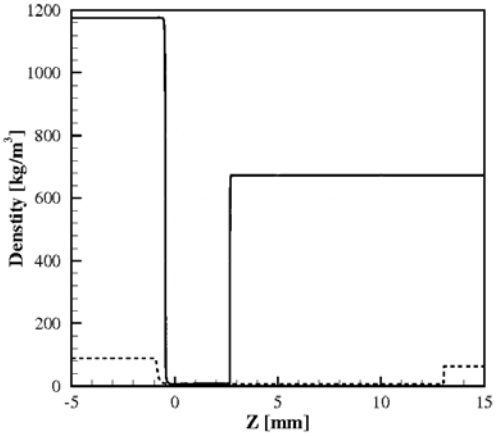

(c) Density

Fig. 10: **Temperature (a), reduced heat release rate distribution (b) and density (c) in partially premixed strained flames formed by a methane / oxygen mixture jet at 110 K (solid) or 300 K (dashed) impinging on a pure oxygen jet at 80 K (solid) or 300 K (dashed) in a 7 MPa environment.** $\phi = 3$**.**

that the merging limit is not reached giving rise to separate reaction layers. A calculation carried out at ϵ_s = 1000 s^{-1} indicates that the two flames merge for the injection temperatures selected for the methane/oxygen mixture. The reduced heat release rate profiles, displayed in Fig. 10(b), also differs from the profile obtained in the supercritical injection case studied previously. The contribution of the nonpremixed flame is much more important in the transcritical state and the endothermic zone is also more important in this case. The rate of conversion in the premixed flame is proportional to the burning velocity, this quantity decreasing in the transcritical case, the contribution of the premixed flame to the heat release rate is diminished and that of the nonpremixed flame is increased. The endothermic zone becomes more and more important as the distance between the two reaction layers is augmented. Density profiles are represented in Fig. 10(c). When injection conditions are transcritical on the two sides, the profile features two strong density gradients which define the thermodynamic evolution of the two streams from low temperature high density to high temperature low density states. The density on the oxygen side takes a value as high as 1176 kg.m^{-3} and on the oxygen / methane mixture 673 kg.m^{-3}

while, in the flame, the density is about 7 kg.m^{-3}. The flames develops in the low-density region and is confined between the two density gradients.

5. Conclusion

Transcritical combustion of partially premixed oxygen and methane is considered in this study. A new library of routines designated as TransChem provides thermodynamic and transport properties over a wide range of pressures and injection temperatures. This includes real gas thermodynamics and anomalies of viscosity and heat conductivity at high pressure. The accuracy of the binary diffusion coefficients model could not be checked because experimental data is lacking. Uncertainty related to the kinetic scheme is documented and shown to influence the premixed side of the flame but to have only a minor effect on the non-premixed flame. Numerical simulations of transcritical strained oxygen/methane flames provide the structure and response to changes in strain rate and premixedness. The flow features a sharp density gradient layer corresponding to transfer of dense transcritical oxygen into lighter supercritical oxygen, a diffusion flame sheet, and a rich premixed flame front. The diffusion flame is backed by the gradient in oxygen density which is established at a point where the mass transferred to the light oxygen region equals the mass consumption rate of oxygen in the diffusion flame. Calculations indicate that changes in equivalence ratio essentially displace the premixed reaction zone with little effect on the non-premixed flame sheet. As the strain rate is increased, the premixed flame moves towards the stagnation plane and the diffusion flame becomes thinner. Combustion regimes are mapped as a function of the strain rate by keeping a constant premixedness and ambient pressure. It is found that merging of the reactive layers takes place at a very high strain rate because the flame is fed by pure oxygen and a non-diluted methane/oxygen mixture. After merging, the flame resembles a non-premixed flame. Its extinction strain rate is large indicating that in practical situations of coaxial injection of transcritical oxygen and methane the flame will be able to sustain the high velocity gradients near the injector exhaust. It is found that the presence of the dense oxygen which exists near the diffusion flame reduces the maximum temperature in this region but this is relatively small and one may conclude that flames established by rocket engines coaxial injectors, keep a standard internal structure and are only weakly influenced by the presence of the transcritical oxygen stream. The density gradient acts somewhat like an impermeable boundary to the reactive region excluding chemical conversion from the dense core. A case of a doubly transcritical partially premixed strained flame where the oxygen and the oxygen / methane mixture are both injected in a transcritical state is also considered. Calculations indicate that the premixed flame is strongly influenced by the temperature of the mixture. The burning velocity is found to decrease with the injection temperature in a nonlinear manner, the decrease being sharper in the transition from a super- to a transcritical state. The premixed flame is stabilized closer to the non-premixed flame. Two density gradients are observed in the two streams and confine the two reaction layers.

Acknowledgments

This research was supported by Snecma, the prime contractor of the Ariane rocket propulsion system, CNES and CNRS in the framework of a collaborative effort with Cerfacs.

References

[1] V. Yang, Proceedings of the Combustion Institute 28 (2000) 925–942.

[2] J. Bellan, Combustion Science and Technology 173 (1-3) (2006) 253–281.

[3] S. Candel, M. Juniper, G. Singla, P. Scouflaire, C. Rolon, Combustion Science and Technology 173 (1-3) (2006) 161–192.

[4] M. Oschwald, J.J. Smith, R. Branam, J. Hussong, A. Schick, Combustion Science and Technology 173 (1-3) (2006) 49–100.

[5] M. Juniper, A. Tripathi, P. Scouflaire, J.C. Rolon, S. Candel, Proceedings of the Combustion Institute 28 (2000) 1103–1109.

[6] G. Singla, P. Scouflaire, C. Rolon, S. Candel, Combustion and Flame 144 (1-2) (2006) 151–169.

[7] G. Singla, P. Scouflaire, J.C. Rolon, S. Candel, Proceedings of the Combustion Institute 31 (2007) 2215–2222.

[8] G. Singla, P. Scouflaire, C. Rolon, S. Candel, Proceedings of the Combustion Institute 30 (6) (2005) 2921–2928.

[9] A. Briones, S.K. Aggarwal, International Journal of Hydrogen Energy 30 (3) (2005) 327–339.

[10] A. Briones, I.K. Puri, S.K. Aggarwal, Combustion and Flame 140 (1-2) (2005) 46–59.

[11] S. Naha, S.K. Aggarwal, Combustion and Flame 139 (1-2) (2004) 90–105.

[12] N. Darabiha, S.M. Candel, V. Giovangigli, M.D. Smooke, Combustion Science and Technology 60 (4-6) (1988) 267–285.

[13] R.D. Lockett, B. Boulanger , S.C. Harding, D.A. Greenhalgh, Combustion and Flame 119 (1-2) (1999) 109–120.

[14] S. Som, S.K. Aggarwal, Combustion Science and Technology 179 (6) (2007) 1085–1112.

[15] G. Ribert, N. Zong, V. Yang, L. Pons, N. Darabiha, S. Candel, Combustion and Flame 154 (3) (2008) 319–330.

[16] L. Pons, N. Darabiha, S. Candel, G. Ribert, V. Yang, Combustion Theory and Modelling ?? (??) (2008) ??–??.

[17] J.C. Oefelein, V. Yang, Journal of Propulsion and Power 14 (5) (1998) 843–857.

[18] J.C. Oefelein, Combustion Science and Technology 178 (1-3) (2006) 229–252.

[19] N. Zong, V. Yang, Combustion Science and Technology 178 (1-3) (2006) 193 – 227.

[20] X.L. Zhu, T. Takeno, J.P. Gore, Combustion Flame 135 (3) (2003) 351–355.

[21] K.G. Harstad, R.S. Miller, J. Bellan, AICHE Journal 43 (6) (1997) 1085–1112.

[22] http://webbook.nist.gov/chemistry/fluid

[23] A. Congiunti, C. Bruno, E. Giacomazzi, Supercritical combustion properties (2003) AIAA Paper No. 2003-0478.

[24] T.H. Chung, M. Ajlan, L.L. Lee, K.E. Starling, Industrial Engineering Chemichal Research 27 (4) (1988) 671–679.

[25] J.F. Ely, H.J.M. Hanley, Industrial Engineering Chemistry Fundamentals 20 (4) (1981) 323–332.

[26] J.F. Ely, H.J.M. Hanley, Industrial Engineering Chemistry Fundamentals 22 (1) (1983) 90–97.

[27] R.J. Kee, G. Dixon-Lewis, J. Warnatz, M.E. Coltrin, J.A. Miller, A Fortran computer code package for the evaluation of gas-phase multicomponent transport properties, Tech. Rep. SAND86-8246, Sandia National Laboratories (1986).

[28] S. Takahashi, Journal of Chemical Engineering (Japan) 12 (1974) 1137–1147.

[29] R. J. Kee, F.M. Rupley, J.A. Miller, Chemkin-2 : A Fortran chemical kinetics package for the analysis of gas-phase chemical kinetics, Tech. Rep. SAND89-8009, Sandia National Laboratories (1989).

[30] H. Meng, V. Yang, Journal of Computational Physics 189 (1) (2003) 277–304.

[31] M. Frenklach, C.T. Bowman, G.P. Smith, W.C. Gardiner, GRI-Mech 3.0, http://www.me.berkeley.edu/gri-mech

[32] P. Lindstedt, Proceedings of the Combustion Institute 27 (1998) 269–285.

[33] W. Juchmann, H. Latzel, D.I. Shin, G. Peiter, T. Dreier, H.R. Volpp, J. Wolfrum, P. Lindstedt, K.M. Leung, Proceedings of the Combustion Institute 27 (1998) 469–476.

[34] L. Pons, N. Darabiha, S. Candel, Combustion and Flame, 152 (1-2) (2008) 218–229.

[35] R.J. Kee, J. Grcar, M. Smooke, J.A. Miller, A fortran program for modeling steady laminar one-dimensiona premixed flames, Report No. SAND85-8240, Sandia National Laboratories (1985)

[36] G. Rozenchan, D. Zhu, C.K. Law, S. Tse, Proceedings of the Combustion Institute 29 (2) (2002) 1461–1470.

[37] G. Jahn, Der zndvorgang in gasgemischen, Oldenbourg, Berlin (1934)

[38] B. Lewis, G. Von Elbe, Combustion, flames and explosion of gases, 3^{rd} edition, Harcourt Brace Jovanovich publishers (1987)

[39] R. Zitoun, B. Deshaies, Combustion and Flame 109 (3) (1997) 427–435.